

2018-10-01

Community managed forests dominate the catchment sediment cascade in the mid-hills of Nepal: A compound-specific stable isotope analysis.

Upadhayay, HR

<http://hdl.handle.net/10026.1/11634>

10.1016/j.scitotenv.2018.04.394

Science of the Total Environment

Elsevier

All content in PEARL is protected by copyright law. Author manuscripts are made available in accordance with publisher policies. Please cite only the published version using the details provided on the item record or document. In the absence of an open licence (e.g. Creative Commons), permissions for further reuse of content should be sought from the publisher or author.

1 Title

2 Community managed forests dominate the catchment
3 sediment cascade in the mid-hills of Nepal: a
4 compound-specific stable isotope analysis

5
6
7 **Hari Ram Upadhayay (1, 4)*, Hugh G. Smith (2), Marco Griepentrog (1, 3), Samuel**
8 **Bodé (1), Roshan Man Bajracharya (4), William Blake (5), Wim Cornelis (6), Pascal**
9 **Boeckx (1)**

10 (1) Isotope Bioscience Laboratory - ISOFYS, Faculty of Bioscience Engineering, Ghent
11 University, Coupure Links 653, 9000 Gent, Belgium, (2) Landcare Research, Private Bag
12 11052, Palmerston North 4442, New Zealand, (3) Biogeoscience, Department of Earth
13 Sciences, ETH Zurich, Sonneggstrasse 5, 8092 Zurich, Switzerland, (4) Aquatic Ecology
14 Center (AEC), School of Science, Kathmandu University, Dhulikhel, Nepal, (5) School of
15 Geography, Earth and Environmental Sciences, Plymouth University, Plymouth, Devon, PL4
16 8AA, UK, (6) Soil Physics Group, Faculty of Bioscience Engineering, Ghent University,
17 Coupure Links 653, 9000 Gent, Belgium

18
19 *Correspondence to:

20 Hari R. Upadhayay

21 hariram.upadhayay@ugent.be or hrgene@gmail.com

22 Phone: +32 9 264 6006; Fax: +32 9 264 6242

23
24 Date of acceptance: 29 April 2018

25 DOI: doi: 10.1016/j.scitotenv.2018.04.394.

26 **Abstract**

27 Soil erosion by water is critical for soil, lake and reservoir degradation in the mid-hills of
28 Nepal. Identification of the nature and relative contribution of sediment sources in rivers is
29 important to mitigate water erosion within catchments and siltation problems in lakes and
30 reservoirs. We estimated the relative contribution of land uses (i.e. sources) to suspended and
31 streambed sediments in the Chitlang catchment using stable carbon isotope signature ($\delta^{13}\text{C}$) of
32 long-chain fatty acids as a tracer input for MixSIAR, a Bayesian mixing model used to
33 apportion sediment sources. Our findings reveal that the relative contribution of land uses
34 varied between suspended and streambed sediment, but did not change over the monsoon
35 period. Significant over- or under-prediction of source contributions could occur due to
36 overlapping source tracer values, if source groups are classified on a catchment-wide basis.
37 Therefore, we applied a novel deconvolutional framework of MixSIAR (D-MixSIAR) to
38 improve source apportionment of suspended sediment collected at tributary confluences (i.e.
39 sub-catchment level) and at the outlet of the entire catchment. The results indicated that the
40 mixed forest was the dominant ($41 \pm 13\%$) contributor of sediment followed by broadleaf
41 forest ($15 \pm 8\%$) at the catchment outlet during the pre-wet season, suggesting that forest
42 disturbance as well as high rainfall and steep slopes interact for high sediment generation
43 within the study catchment. Unpaved rural road tracks located on flat and steep slopes (11 ± 8
44 and $9 \pm 7\%$ respectively) almost equally contributed to the sediment. Importantly, agricultural
45 terraces (upland and lowland) had minimal contribution (each $<7\%$) confirming that proper
46 terrace management and traditional irrigation systems played an important role in mitigating
47 sediment generation and delivery. Source contributions had a small temporal, but large spatial,
48 variation in the sediment cascade of Chitlang stream. D-MixSIAR provided significant
49 improvement regarding spatially explicit sediment source apportionment within the entire
50 catchment system. This information is essential to prioritize implementation measures to
51 control erosion in community managed forests to reduce sediment loadings to Kulekhani

52 hydropower reservoir. In conclusion, using compound-specific stable isotope (CSSI) tracers
53 for sediment fingerprinting in combination with a deconvolutional Bayesian mixing model
54 offers a versatile approach to deal with the large tracer variability within catchment land uses
55 and thus to successfully apportion multiple sediment sources.

56

57 **Keywords**

58 fatty acids, compound-specific stable isotope (CSSI) analysis, isotope mixing model,
59 deconvolutional approach, MixSIAR

60

61

62

63

64

65

66

67

68

69

70

71

72

73

74

75

76 **1 Introduction**

77 Soil erosion by water is of paramount importance for Nepal because of its adverse
78 impacts on soil quality (Acharya et al., 2008; Gardner and Gerrard, 2003), aquatic life in lakes
79 and rivers, and reservoir capacity (GoN/EbA/UNDP, 2015). Degradation of soils through
80 water erosion is one of the key issues affecting agriculture in the mid-hills of Nepal (Acharya
81 et al., 2008; von Westarp et al., 2004). Therefore, it is also considered a major threat to food
82 security and potentially puts rural mountain communities, which rely on the economy of local
83 agriculture and subsistence farming, at risk. Moreover, river, lake and reservoir siltation
84 represent a major challenge and its effect can be environmentally and economically
85 detrimental in terms of water and energy security of the region (GoN/EbA/UNDP, 2015).
86 Human activity, combined with natural factors such as steep slopes, fragile geology and
87 intensive monsoon rains, provides conditions for extensive soil loss and is intrinsically linked
88 with catchment degradation. Given the complex interaction with human activities and
89 environment, the nature and extent of soil erosion is highly variable in space and time.
90 Upstream erosion control such as improvements in terracing, low-till agriculture and
91 reforestation have been the focus to mitigate erosional losses (Tiwari et al., 2009) and to
92 reduce sedimentation of reservoirs and lakes in the mid-hills of Nepal. However, questions
93 remain about the extent to which specific land-use types prevent or exacerbate erosion and
94 land degradation in the context of current and future projected agricultural intensification
95 (Bahadur, 2012) as well as changing rainfall patterns in the mid-hills of Nepal (Bookhagen,
96 2010). Answering these questions is critical to developing a strategy for preventing soil loss
97 and reducing siltation of lakes and reservoirs.

98 Information on land use-based sediment sources can considerably enhance our
99 understanding of sediment origin. Sediment source fingerprinting by compound-specific
100 stable isotope (CSSI) analyses of fatty acids (FA) has been used as a reliable method to

101 investigate land use-based sediment sources at the catchment scale (Gibbs, 2008; Upadhayay
102 et al., 2017). The premise of the CSSI sediment source fingerprinting approach is that soil
103 from different land uses can be distinguished based on isotopic composition (^{13}C) of FAs
104 bound to soil particles (Gibbs, 2008; Upadhayay et al., 2017). Fatty acids are biosynthesized
105 by higher plants, delivered to soils and thereby labelling the soil with FAs having a specific
106 $\delta^{13}\text{C}$ signature ($\delta^{13}\text{C}$ -FAs). Fatty acids associated with soil particles, get mixed during
107 downstream sediment transport. Isotope mixing models using $\delta^{13}\text{C}$ -FA values of sources and
108 sediment sinks offer the possibility of estimating the relative contribution of sources to the
109 sediment (Upadhayay et al., 2017). These estimates can be used to identify differences in
110 sediment sources on spatial (e.g. sub-catchments) and temporal (e.g. seasons) scales and to
111 suggest catchment remediation measures (Mukundan et al., 2012).

112 Sediment fingerprinting has been successfully applied as a tool to gain insights into
113 sediment dynamics at a river basin scale in catchments all over the world since the 1970s
114 (Mukundan et al., 2012; Walling, 2013). Spatio-temporal variation of sediment source
115 apportionment has received increasing attention (Cooper et al., 2015; Vale et al., 2016;
116 Vercruyssen et al., 2017), because primary sediment sources are site-specific and vary within a
117 catchment (Koiter et al., 2013a; Stewart et al., 2015). In essence, changes in rainfall pattern
118 and intensity, and land cover change in both natural (e.g. loss of leaf cover in a deciduous
119 forest during winter) and agricultural systems (e.g. bare soil due to changing cropping patterns)
120 cause marked temporal variations in sediment sources and dynamics (Merz, 2004). Often the
121 fingerprinting signature of different land uses (sources) is only weakly expressed by the
122 applied tracer techniques (Pulley et al., 2017). A possible solution lies in alternative sampling
123 approaches, such as (1) ‘compositional evolution’ (Hardy et al., 2010), whereby sources, as
124 well as sediment, are sampled along the river, or (2) ‘confluence-based sediment
125 fingerprinting’ (Vale et al., 2016), whereby upstream sediment samples are taken as a proxy

126 for sub-catchment sediment signature in order to evaluate relative source contributions for
127 larger catchments. The former approach does not account accurately for sub-catchment
128 contributions as well as local variability of tracers, while the latter approach lacks the ability
129 to provide information on the specific sediment sources within sub-catchments (Vale et al.,
130 2016). Very limited work has been done to identify land use-based sediment sources and to
131 estimate their relative contributions as a function of land use within sub-catchments using
132 CSSI tracers. In this study, we applied the CSSI sediment source fingerprinting approach
133 within a representative catchment and its sub-catchments in the mid-hills of Nepal. The
134 objectives were (a) to determine the relative contributions of generic sediment sources (i.e.
135 catchment-wide source groups) to sediment loads and (b) to evaluate how source
136 contributions to the catchment sediment cascade change on a spatio-temporal basis.

137

138 **2 Material and methods**

139 **2.1 Catchment description**

140 The study was conducted in the Chitlang catchment (23 km²), which drains into the
141 Kulekhani Hydropower Reservoir (also known as Inra Sarobar), located in the mid-hills of
142 Nepal (Fig. 1). This catchment is mainly dominated by forests (>70%), which can be
143 categorized into broadleaf forest (25%), mixed forest (40%) and pine forest (6%) (Table A.1).
144 The agricultural systems consist of (a) lowland terraces (6%): bunded irrigated levelled
145 terraces called “Khet” and (b) upland terraces (23%): unbunded rain-fed levelled terraces
146 called “Bari”. Rice is predominantly grown in lowland terraces during the peak monsoon
147 season (July to September). Wheat and other commercial vegetables are dominant during the
148 winter season in the lowland terraces. Similarly, in the upland terraces, maize may be grown
149 as a monoculture or intercropped with finger millet and other vegetables (potato, cabbage,
150 cauliflower, legumes). Most cropland is either privately owned or rented and receives

151 inorganic fertilizer and farmyard manure, while forests are owned and managed by
152 community forest user groups (CFUs).

153 The catchment has a rugged terrain with an elevation ranging from 1515 to 2555 m and
154 an average slope gradient of 44% (Fig. 1b and Fig. 2a). Less than 27% of the area has a slope
155 <30%. Land use is closely related to the slope gradient of the catchment (Fig 1). Slopes <25%
156 are dominated by agriculture, while lowland terraces are found particularly at the bottom of
157 the hills on relatively flat land (<15% slope gradient) near stream banks (Fig. 1b). Forests
158 dominate on steeper slopes (>25%). The catchment is characterized by monsoon climate, with
159 two distinct seasons: summer monsoon and dry winter (Fig. 3). Annual average precipitation
160 is ~1750 mm (maximum 2386 mm and minimum 1182 mm according to data from 1980 to
161 2015). Most precipitation (circa 77%) occurs during the peak monsoon season between June
162 and September (Markhu Gaun station (index no 0915), Department of Hydrology and
163 Meteorology (DHM), Government of Nepal). Additionally, 16% of precipitation occurs in
164 early (April and May) and late monsoon (October and November) and 7% during the dry
165 winter period (between December and March).

166 The soils in the catchment are classified as Cambisol (Dijkshorn and Huting, 2009)
167 developed on Phulchoki sub-group which consists of Chitlang (dominant in the headwaters),
168 Chandragiri, Sopyang and Tistung formation (Dhital, 2015). Surface soil has a silt-loamy
169 texture with significantly higher soil erodibility (K) on cropland compared to forest land
170 (Upadhyay et al., 2014). However, average surface soil loss from cropland with gentle slopes
171 of 14-20% is estimated to be below $2.5 \text{ t ha}^{-1} \text{ yr}^{-1}$ (Sthapit and Balla, 1998). Water erosion
172 supplies sediment to the 9.7 km long Chitlang stream (drainage density: $\sim 4.1 \text{ km km}^{-2}$) and to
173 the Kulekhani reservoir (Fig 1a). This reservoir is of national importance as it is the only
174 functional seasonal reservoir of Nepal and provides 25-30% of the national electricity demand

175 during the dry season (NEA, 2016). The Kulekhani reservoir lost circa 40% of its water
176 storage capacity in 30 years of operation due to siltation (Shrestha, 2012).

177

178 **2.2 Source soil and sediment sampling**

179 Potential sediment sources and sediment sampling locations were identified via a land
180 use map digitized from *Google Earth* and a topographical map obtained from the Department
181 of Survey, Government of Nepal as well as a reconnaissance survey in 2013. Identified land-
182 uses were divided into five generic potential sediment source (primary) groups: broadleaf
183 forest (BLF), mixed forest (MF), pine forest (PF), upland terraces (UP) and lowland terraces
184 (LL) (Fig. 1a, Table A.1). Unpaved road tracks (RT) were considered as secondary sediment
185 source since RT do not generate carbon isotopic signature, but rather integrate the signatures
186 of the adjacent land uses. The sampling strategy was designed to take the distribution of land
187 uses, especially the patchy agricultural practices (i.e. smallholder farmers with great
188 variability in crop choice, agronomic practices and inputs) across the catchment, topographic
189 locations and sub-catchments into account. Multiple composite soil samples from different
190 spatial locations belonging to each land use were obtained according to natural and
191 management factors, and accessibility. Each composite soil sample was composed out of a
192 pool of 15 random subsamples (2 cm top soil obtained using a stainless steel corer with 7.5
193 cm internal diameter). The composite samples included loose soil in the exposed area as well
194 as fresh deposits at the base of each land use clearly showing recent movement of soil due to
195 overland flow. In case of RT, source samples were taken from their surface and in road-side
196 channels. Stream-banks were not sampled as a separate source because of high gravel and
197 boulder content dominating the substrate as well as a high vegetation cover along the Chitlang
198 stream and its tributaries (Fig. A.1). Landslides were not observed in the catchment
199 throughout the study period (2013-2015).

200 Two different types of sediment samples were collected between 2013 to 2015 and
201 2014 to 2015, i.e. (1) deposited streambed sediment (Fig 2b) and (2) suspended sediment (Fig.
202 2c), respectively. Both types of sediment samples were retrieved during the early wet (EW;
203 March-May), mid wet (MW; June-August) and late wet (LW; September-October) periods to
204 capture the range of flow conditions that occur over the years and to understand the spatio-
205 temporal variation of sediment sources (Fig. 3). Early wet season is the critical time for soil
206 loss from cropland in the mid-hills of Nepal. Each streambed sediment sample comprised 10-
207 15 subsamples (grabs/scrapings) collected from the floodplain, gabion dam and interstices
208 between larger clasts using a flat trowel over approximately 250 m distance at the outlet (M6)
209 of the catchment (Table 1, Fig. 1a). Suspended sediment was sampled with time-integrated
210 mass-flux samplers (TIMS) (Fig. 2c) that were deployed at specific locations as shown in Fig.
211 1a. These sediment traps were constructed from PVC pipes (1 m length, 110 mm diameter,
212 following the design of Phillips et al.,(2000). Two replicated sediment traps were installed at
213 each sampling location (except for the outlet, M6, of the Chitlang stream where six replicated
214 TIMS were installed) (Fig.1a). Moreover, suspended sediment was collected up- and
215 downstream of stream confluences to investigate sediment inputs from individual sub-
216 catchments (Fig. 1a, Table 1). Upstream samples were collected very close to (~10 m) the
217 confluence point while downstream samples were collected approximately 200 to 250 m
218 downstream of the confluence.

219 Additionally, during the rising and falling stages of a large runoff event on 14 to 15
220 August 2014 (116 mm of rain fell over a period of 24 hours), suspended sediment was
221 sampled from bulk water samples into 150 L Nalgene containers at the terminus of the
222 Chitlang stream (M6, Fig. 1a). Sediment was separated by decantation following a settling
223 period in a dark cool room (2-3 days). Additionally, suspended sediment samples were
224 retrieved from TIMS at the outlet of the Chitlang stream covering a duration of 35 days (25

225 April to 30 May) over a period of 30 aftershocks of local magnitude higher than 5.0 M
226 following the Gorkha earthquake (7.8 M) on 25 April 2015. During this period, the total
227 rainfall was 68 mm with one event having 34 mm rain during less than 24 hours. All soil and
228 sediment samples were air-dried, crushed with a steel roller on a steel tray (Gibbs, 2013) and
229 sieved at 2 mm prior to further analyses.

230

231 **2.3 Total organic carbon (stable isotope) analysis**

232 Bulk organic carbon contents and stable carbon isotope composition ($\delta^{13}\text{C}$) of source
233 soils and sediment samples were measured using an elemental analyser (ANCA-SL, SerCon,
234 Crew, UK) coupled to an isotope ratio mass spectrometer (20-20, SerCon, Crew, UK). A mass
235 of 10 to 15 mg grinded sample was transferred into tin capsules and loaded into an auto-
236 sampler. Wheat flour ($\delta^{13}\text{C} = -27.21 \pm 0.13\%$) calibrated against the IAEA-CH-6 standard
237 was used as laboratory standard and stable carbon isotope values were expressed as $\delta^{13}\text{C}$
238 values relative to the Vienna Pee Dee Belemnite (VPDB) international reference standard.

239

240 **2.4 Fatty acid extraction and carbon isotope measurement**

241 Lipids were extracted from source soils and sediment samples with accelerated solvent
242 extraction (ASE 350 Dionex) using dichloromethane:methanol (9:1, v/v) at 100°C and
243 1.3×10^7 Pa for 5 min in 3 cycles (30 mL cells, 60 % flush volume). The volume of total lipid
244 extract was reduced by evaporation at reduced pressure and neutral and acidic compounds
245 were separated using solid phase extraction on aminopropyl-bonded silica gel columns
246 according to Blake et al. (2012). The acid fraction was methylated with methanolic HCl
247 (Ichihara and Fukubayashi, 2010) of known carbon isotopic composition ($\delta^{13}\text{C} = -40.78 \pm$
248 0.33%) and an internal standard (C_{17} FA, heptadecanoic acid) for FA quantification was
249 added to each sample prior to analysis. Fatty acid methyl esters (FAME) were subsequently
250 analysed by capillary gas chromatography-combustion-isotope ratio mass spectrometry (GC-

251 C-IRMS; Trace GC Ultra interfaced via a GC/C III to DeltaPLUS XP, Thermo Scientific,
252 Bremen, Germany). FAMES were identified based on the retention time, while peak purity
253 and confirmation of identity was done using a parallel GC-MS measurement. An in-house
254 prepared FAME mixture (C₂₀ - C₃₀ FAs), traceable to IAEA-CH6 (cumulative uncertainty on
255 the VPDB scale was < 0.2‰), was injected every six sample injections as a reference for ¹³C
256 isotope ratio measurement of FAMES. Sample analyses were run in duplicate or triplicate
257 with a standard deviation lower than 0.4‰. Isotope ratios are expressed as δ¹³C values in per
258 mill relative to the VPDB standard. The contribution of the δ¹³C values of the added methyl
259 group was subtracted from the δ¹³C value of the analysed FAME to determine the δ¹³C values
260 of the FAs in the source and sediment samples (see equation in Griepentrog et al., 2015).
261 Cumulative uncertainty on VPDB scale for the FA was < 0.6‰. Long-chain even carbon
262 numbered fatty acids (C₂₂ - C₃₂) were used for further analysis.

263

264 **2.5 Data processing and deconvolutional-MixSIAR formulation**

265 Two tracer sets were defined to evaluate their capacity in discriminating between the
266 potential generic sediment sources (land uses). The first set comprised the δ¹³C values of
267 long-chain saturated fatty acids (C₂₂-C₃₂); in the second set, the bulk soil δ¹³C value was
268 included together with the δ¹³C-FA (C₂₂-C₃₂) values. Discriminant analysis (DA) is a
269 supervised statistical algorithm that derives an optimal separation between sources established
270 a priori by maximizing between-source variances while minimizing within-source variance
271 (Huberty and Olejnik, 2006). A prediction matrix was used to assess the performance of DA.
272 A plot of individual scores was used to visualize how the first two discriminant functions (e.g.
273 LD1 and LD2) accounted for separation among land uses. The Mahalanobis distance, a
274 measure of distance between two points in the space defined by two or more correlated

275 variables, was also used as auxiliary information to evaluate the capacity of tracer sets to
276 discriminate between the land uses.

277 First, the apportionment of land use sources contributing to sediment was estimated
278 using FA tracers from catchment-wide pooled source groups as input for a concentration-
279 dependent mixing model (pooled-MixSIAR). MixSIAR is a Bayesian isotope mixing model
280 (Stock and Semmens, 2013) for estimating the contribution of end-members (i.e. sources)
281 using the tracer content of sources and sediment with model error (residual and process error)
282 (Parnell et al., 2010; Upadhayay et al., 2017). Before starting the un-mixing process with
283 MixSIAR, conservativeness of the tracers was tested using the point-in-ellipsoid approach
284 (Jackson, 2016). Briefly, a 95% prediction ellipse is made from source tracer data (i.e. 95% of
285 the source data are included in the ellipse) and transformed into a perfect circle, centred
286 around the origin using the covariance matrix. Such transformation was also applied to
287 sediment tracer data points in order to determine whether or not sediment samples are within
288 the radius of the source data circle and are hence conservative. This was done considering all
289 tracers i.e. dimensions in a hyperspace. Subsequently, concentration-dependent MixSIAR was
290 formulated with selected FAs, using a residual error term, with the season (sediment sampling
291 periods) as a fixed effect, and no prior information. A concentration-dependent mixing model
292 is essential for accurate quantification of sediment source contributions (Upadhayay et al.,
293 2018). Residual error accounts for unknown sources of variability in the sediment
294 (Upadhayay et al., 2017). The Markov Chain Monte Carlo (MCMC) parameters in MixSIAR
295 were set as follows: number of chains = 3, chain length = 3,000,000, burn = 1,500,000, thin
296 =500. Convergence of mixing models was evaluated using the Gelman-Rubin diagnostic,
297 rejecting the model output if any variable was above 1.0, in which case the chain length was
298 increased. Furthermore, a diagnostic matrix plot of posterior source contribution was used to
299 evaluate the quality of source discrimination. Mean proportional contributions are reported

300 along with uncertainty and 90% credible interval (CI). A CI (Bayesian form of confidence
301 intervals) is an interval in the domain of the posterior density function (PDF) used to
302 determine uncertainty, i.e., the probability that the true source contribution lies within the
303 interval.

304 Second, a novel “deconvolutional MixSIAR” (D-MixSIAR) framework was used to
305 apply land use-based source fingerprinting within the catchment stream network structure. In
306 this approach, sub-catchment-specific sources were first unmixed against sediment from
307 individual tributaries (e.g. M1 and M2, Fig. 1a), and then tributaries were unmixed against
308 sediment after a confluence of both tributaries (e.g. M3, Fig. 1a). Posterior proportional
309 contributions of each basin-wide source were then deconvoluted. This approach allows
310 estimation of the weighted distribution of land use contributions to nested downstream
311 sediment sampling locations. D-MixSIAR requires data input to estimate land use source
312 contributions to stream sediment within each sub-catchment, and the sub-catchment
313 contributions to sediment collected downstream of the confluence of streams draining the sub-
314 catchments. Sediment source apportionment per sub-catchment was done by considering
315 source samples within the contributing sub-catchments, upstream of the suspended sediment
316 collection site. Based on field observations and variability of the CSSI signature, it was
317 decided to subdivide the RT samples from the Dandakharka sub-catchment (Fig. 1a) into sub-
318 groups, namely RT-1 (RT samples from relatively steep areas inside BLF) and RT (RT
319 samples from the flatter part of the catchment), while UP samples comprised sub-group UP
320 and UP-E (= upland agriculture encroached into BLF). All statistical analyses and unmixing
321 modelling were done using R software (version 3.3.1, R Core team, 2016) with SIBER
322 (Jackson, 2016), MASS (Venables and Ripley, 2002), HDMD (McFerrin, 2013) and
323 MixSIAR (Stock and Semmens, 2013) packages in the library.

324

325 **3 Results**

326 **3.1 Discrimination of generic sediment sources**

327 Exploratory statistical analysis to assess the potential discriminative power of applied
328 isotopic tracers is important. Discriminant analysis (DA) based on $\delta^{13}\text{C}$ -FA shows that the
329 two dimensions accounted for >90% of the variance (LD1 = 57.6%, LD2 = 33.6%) as shown
330 in Fig. 4. Group centroids show multivariate mean values, visualising the separation of source
331 groups relative to the functions. All land use pair-wise Mahalanobis distances from the
332 centroid were highly significant except for the pairs BLF-MF, LL-RT and UP-RT (Table 2).
333 Results showed that BLF-MF was most similar in terms of $\delta^{13}\text{C}$ -FA values. The discriminant
334 analysis further showed that RT is positioned centrally to all other sediment sources (Fig. 4)
335 with a high spread (Fig. A.2) reflecting the presence of road tracks across different land uses.
336 The classification based on DA allowed for 65% total correct classification with some source
337 groups displaying clear discrimination (e.g. PF), while others with greater similarity in $\delta^{13}\text{C}$ -
338 FA values proved more difficult to discriminate. The main misclassification is related to the
339 RT, BLF and MF with the lowest correct classification of 11, 45 and 47%, respectively (Table
340 A.2). The inclusion of bulk $\delta^{13}\text{C}$ into the tracer set did not change the classification accuracy
341 of the sources significantly (data not shown).

342

343 **3.2 Proportional contributions of different land uses to catchment-wide** 344 **sediment during monsoon season**

345 Different land use contributions to sediment at the outlet of the Chitlang stream (M6,
346 Fig.1a) were estimated from catchment-wide pooled source groups using MixSIAR (pooled-
347 MixSIAR). Point-in-ellipsoid analysis of isotopic tracers demonstrated that the majority of
348 sediment samples (96 and 94% of suspended and streambed sediment, respectively) fell
349 within the source tracer mixing polygon and hence can be considered as conservative.
350 However, we did not remove any sediment sample that failed the point-in-polygon test in

351 further modelling, since MixSIAR can handle to some extent unknown variations in sediment
352 $\delta^{13}\text{C}$ -FAs via the residual error term (Semmens et al., 2009; Upadhayay et al., 2017). Mixing
353 modelling results demonstrated the substantial variability and uncertainty in the estimated
354 source contribution to sediment (Fig. A.3) with strong negative correlations in posterior
355 source contribution (Fig. A.4) due to the overlap of tracer values between land uses (Fig. 4,
356 Fig. A.2 a-f) while considering catchment-wide (generic) sediment sources. For example, a
357 very strong negative correlation (-0.97) between the posterior probability of BLF and MF
358 contributions was observed in suspended sediment, while, in the case of streambed sediment,
359 posterior probability distributions of BLF were negatively correlated with MF (-0.57) and RT
360 (-0.54). A negative correlation between posterior probabilities of two sources indicates
361 collinearity and thus a low ability of tracers to discriminate between sources. Furthermore,
362 credible intervals of functionally related sources were wide and overlapping. Therefore,
363 probabilities associated with source contributions were aggregated posteriori, i.e. deciduous
364 forest (DF) was formed from BLF and MF while LL and UP were aggregated to form
365 agriculture (AG), to estimate the proportional contribution of meaningful functional source
366 groups to the different types of sediment i.e. suspended, streambed and events.

367 Figure 5 summarizes the source apportionment results (after aggregating posterior
368 probability of source) of sediment samples that were collected at the outlet (M6) of the
369 Chitlang stream. The estimated mean relative contribution of each source to the suspended
370 sediment indicated that DF was the dominant source during the early, mid and late wet season,
371 with a 90% CI ranging between 90 and 99%, followed by AG ranging between 0.3 and 4%.
372 Similar to the suspended sediment, results for streambed sediment in the Chitlang stream
373 indicated that it was predominantly derived from DF (average contribution of 62, 79 and 68%
374 in early, mid and late wet season, respectively), followed by AG (18, 9 and 15%) and RT (14,
375 5 and 8%) which indicates that surface erosion from agricultural terraces is a minor source

376 (Fig. 5). For streambed sediment, seasonality was observed for DF with a significantly higher
377 contribution in the mid wet compared to early and late wet-periods (79% versus 62 and 68%,
378 respectively). Source apportionment results did not substantially change in both sediment
379 types i.e. suspended and streambed between the cases where bulk $\delta^{13}\text{C}$ was included ($\delta^{13}\text{C}$ -
380 FA (C₂₂-C₃₂) + $\delta^{13}\text{C}$ -bulk) and the cases where bulk $\delta^{13}\text{C}$ was not included ($\delta^{13}\text{C}$ -FA (C₂₂-
381 C₃₂)) as tracer (Fig. A.3). Hence further discussion and conclusions are based on the results of
382 $\delta^{13}\text{C}$ -FA tracer set.

383 Additionally, identification and apportionment of sediment sources during intense
384 rainfall events provide the basis for a detailed assessment of critical land uses that contribute
385 substantial amounts of sediment at the catchment scale. Table 3 presents information on the
386 overall mean relative contribution of sources to suspended sediment samples collected at the
387 outlet of the Chitlang catchment during a high rainfall event (14-15 August 2014) and the
388 geodynamically active period (after 7.8 M Gorkha earthquake in 2015). For the rainfall event,
389 DF contributed an average (\pm standard deviation) of $76 \pm 10\%$, while AG and RT contributed
390 equally with an average contribution of $10 \pm 6\%$ and $9 \pm 8\%$ respectively. Furthermore,
391 posterior probability distributions of sediment sources during the period of frequent
392 aftershocks (25 April - 30 May 2015) showed that the majority of sediment also originated
393 from DF ($74 \pm 11\%$), followed by AG ($11 \pm 7\%$) and RT ($10 \pm 9\%$).

394

395 **3.3 Sediment contribution by sub-catchments using deconvolutional** 396 **MixSIAR**

397 The variability of $\delta^{13}\text{C}$ -FAs and organic carbon for sediment sources and sediments of
398 individual sub-catchments (Table 1) indicated that potential sediment sources have unique
399 $\delta^{13}\text{C}$ -FAs values (Fig. A.5 and Fig. A.6). Sediment source contributions for different
400 tributaries of the Chitlang stream were estimated (Fig. 6) with source samples from the

401 respective tributary's sub-catchments. Source contributions were found to vary by sub-
402 catchment temporally. Sediment from the Dandakharka sub-catchment (M1, Fig. 1a)
403 originated from BLF (average contribution of 43, 31 and 25% in the early, mid and late wet
404 season, respectively), followed by RT-1 (27, 33, 33% in the early, mid and late wet season),
405 UP-E (10, 13, 14% in the early, mid and late wet season), MF (8, 11, 15 % in the early, mid
406 and late wet season), while other sources showed only minor contributions (<5%) (Fig. 6).
407 Sediment from the sub-catchment Kharka (M2, Fig. 1a) was dominated by MF 74, 87 and
408 75% during early, mid and late wet season, respectively. Mixing model estimation suggested
409 that sediment samples collected after the confluence of M1 and M2 i.e. M3 comprised overall
410 mean (\pm standard deviation) contributions of 74 ± 18 , 78 ± 20 to $83 \pm 17\%$ during early, mid
411 and late wet-periods, respectively, from Dandakharka (M1) and 26 ± 18 , 22 ± 17 to $17 \pm 17\%$
412 during early, mid and late wet season, respectively, from Kharka (M2) (Table 4). Similar to
413 M2, Chhabugaun tributary sediment (M4, Fig. 1a) predominantly originated from MF
414 (average contribution 87, 95 and 87% during early, mid and late wet season, respectively).
415 The average contributions from the Upper-Chitlang (= M1 + M2) sub-catchments to sediment
416 samples collected after the Kapu confluence (M5, Fig. 1a) were 71, 64, to 74% during early,
417 mid and late wet seasons, respectively. Tributary sub-catchment contributions are generally in
418 agreement with catchment size, steepness and level of disturbance.

419 Combination of these sub-catchment estimates with the source contribution estimates for
420 each sub-catchment provides the basis for determining weighted sediment contributions for
421 M3, M5 and M6 within the D-MixSIAR framework. Three sources namely BLF, MF and RT-
422 1 almost equally contributed to M3 sediment: BLF contributed 32 ± 17 , 24 ± 15 and $21 \pm 13\%$
423 followed by MF by 25 ± 14 , 27 ± 18 and $25 \pm 16\%$ and RT-1 by 20 ± 17 , 26 ± 23 and $27 \pm$
424 24% during early, mid and late wet season, respectively. In contrast, for M5 sediment, MF
425 contributed to almost half of the sediment (43 ± 15 , 52 ± 18 , $41 \pm 18\%$ for early, mid and late

426 wet season, respectively), followed by an almost equal contribution from BLF (23 ± 12 , $15 \pm$
427 11 , $15 \pm 11\%$ for early, mid and late wet seasons, respectively) and RT-1 (14 ± 13 , 17 ± 16 ,
428 $20 \pm 14\%$ for early, mid and late wet season, respectively). In the case of the whole Chitlang
429 catchment (M6), the majority of sediment originated from MF (41 ± 12 , 47 ± 18 , $38 \pm 14\%$
430 for early, mid and late wet season, respectively) with almost equal contributions from BLF
431 (15 ± 8 , 10 ± 7 , $9 \pm 7\%$ for early, mid and late wet season, respectively), RT (11 ± 8 , 7 ± 6 , 10
432 $\pm 8\%$ for early, mid and late wet season, respectively) and RT-1 (9 ± 8 , 11 ± 10 , $13 \pm 12\%$ for
433 early, mid and late wet season, respectively), while LL, UP, PF and UP-E contributed the
434 lowest amounts of sediment (Fig. 6, Fig. A.7). RT-1 was highest contributor in the upstream
435 during mid and late-wet season and their contribution also gradually decreases downstream
436 (Fig. A.7). The combined contributions from RT and RT-1 showed that unpaved road tracks
437 were responsible for the second-largest proportion of M6 sediment after DF (BLF and MF).
438 MF contributions gradually increased from upstream to downstream, while sediment
439 contribution of BLF gradually decreased in the same direction (Fig. A.7). In most sediment,
440 the 90% CI of source contributions showed wide ranges (this was especially true for RT-1,
441 MF, BLF and UP-E), whereas the 90% CI of LL, RT, UP and PF were narrower (Fig. 6).

442

443 **4 Discussion**

444 **4.1 Sediment source discrimination**

445 Establishment of robust discrimination between $\delta^{13}\text{C}$ -FAs values of sediment sources is
446 a key requirement for accurate source apportionment (Davis et al., 2015). An overlap was
447 observed to some extent as well as source groups with large within-group variability (e.g. MF
448 and RT, Fig. 4). This explains why mixing modelling yielded a high negative correlation
449 between the contributions of these sources, irrespective of sediment types (Fig. A.4) and
450 tracer sets. This was most notable between BLF and MF, and also between MF and RT. The

451 large negative correlation in posterior source contribution indicates that these sources are
452 similar to each other in terms of tracer isotope values, which indicates that only one of both
453 sources can actually contribute to the sediment mixture at a specific time (Stewart et al., 2015).
454 Similar $\delta^{13}\text{C}$ -FA values were expected in BLF and MF, since MF is dominated by broadleaf
455 and pine trees are relatively sparse in MF and thus less likely influence $\delta^{13}\text{C}$ -FA values. Soils
456 under BLF and MF were characterised by $\delta^{13}\text{C}$ -FA values for C3 plants (Diefendorf et al.,
457 2015). The LL and UP terraces are characterised by intense cultivation of varying crop types
458 (i.e. cereal-legume/vegetable rotation) and soil management practices (tillage and farm yard
459 manure (FYM) application), which may have caused high variation in $\delta^{13}\text{C}$ -FA values (Fig.
460 A.2), especially due to mixing of C3 (rice, wheat, potato, beans) and C4 (maize, millet) plants.
461 Removal of above ground biomass from agriculture fields is a common practice in the
462 catchment. Instead of crop biomass, application of highly variable amounts of FYM, which is
463 produced from crop biomass, leaf litter and pine needles, may introduce the isotopic signature
464 of forest-derived FAs into agriculture fields and thereby lead to an increase in source
465 variability (Jandl et al., 2007; Jandl et al., 2005). Additionally, LL receives sediment during
466 flooding (Brown et al., 1999), which might also redistribute FA isotopic signatures from UP
467 to LL. This is partially responsible for similar variation and overlapping source $\delta^{13}\text{C}$ -FAs
468 values (Fig. A.2), despite the cultivation of plants with different photosynthetic pathways as
469 major crops. Overlap and large within-source variability of $\delta^{13}\text{C}$ -FAs values of sources are
470 considered important challenges in the application of isotope mixing models (Parnell et al.,
471 2010). They are expected to result in an increased uncertainty in the estimated source
472 contributions (Phillips and Gregg, 2001; Upadhayay et al., 2017). The a priori combination of
473 sources (BLF and MF) as 'deciduous forest' gave similar results as the sum of the
474 contributions of BLF and MF in the original analysis, i.e. posteriori aggregation of sources

475 (data not shown). This suggests that although the tracers are not able to discriminate between
476 two functional sources, they can estimate their collective contribution to the sediment.

477 For both sediment types (suspended and streambed), the sediment source contributions
478 did not change significantly when bulk $\delta^{13}\text{C}$ was added as an additional tracer (Fig. A.3).
479 Despite the abundant use of soil and sediment bulk $\delta^{13}\text{C}$ in sediment tracing research (Collins
480 et al., 2013; Fox and Ford, 2016; Fox and Martin, 2015; Fox and Papanicolaou, 2007; Lacey
481 et al., 2015), there is no strong evidence that bulk soil $\delta^{13}\text{C}$ behaves conservatively (Collins et
482 al., 2014; McCarney-Castle et al., 2017). The non-conservative behavior of bulk sediment C
483 isotopes is possibly due to fractionation during organic matter decomposition (Benner et al.,
484 1987; Fine and Carter, 2013). Furthermore, aquatic vegetation and freshwater autotrophs (e.g.
485 algae) easily contaminate the sediment potentially altering the bulk isotope signature of the
486 sediment, thereby confounding the interpretation of the source of eroded material. Despite
487 these risks, several studies suggest the use of bulk isotopes as primary tracers in isotope
488 mixing models during CSSI sediment source fingerprinting (Blake et al., 2012; Gibbs, 2008;
489 Gibbs, 2013; Hancock and Reville, 2013). Our results suggest that bulk C isotopes should not
490 be used in CSSI sediment source fingerprinting without evidence to support their conservative
491 behavior.

492

493 **4.2 Source contributions for different types of sediment**

494 Both suspended and streambed sediment has been widely adopted in sediment source
495 fingerprinting research (Collins et al., 2017; McCarney-Castle et al., 2017; Wilkinson et al.,
496 2015). Bayesian modelling results supported the qualitative graphical analyses (Fig. 4) and
497 also suggested DF (combined BLF and MF) as a primary source, with very small inter-
498 seasonal variability in its relative contributions to suspended sediment compared to streambed
499 sediment (Fig. 5). Differences in source composition between suspended and streambed

500 sediment have been reported in other studies (Koiter et al., 2013b; Lamba et al., 2015) that
501 suggest both should be sampled to effectively understand sediment sources. However,
502 variations in the estimated DF contribution to sediment types (Fig. 5) do not alter the broad
503 conclusion that hillslope forest represents a primary sediment source within Chitlang
504 catchment. Whilst this partial conclusion is based on the modelling of tracer data of generic
505 (catchment-wide pooled) sediment sources and the plausible assumption that suspended
506 sediment is dominated by newly delivered sediment from land surface sources (stream bed
507 deposition and remobilisation of sediment is less likely in fast flowing mountain streams),
508 sediment source apportionment within an individual sub-catchment should be considered to
509 better understand the origin of sediment at a higher spatial resolution (section 4.3). Moreover,
510 sediment core analysis from the reservoir could be used to predict the long-term variation of
511 sediment source contributions, which is lacking in this study. Therefore, we concentrate on
512 suspended sediments in the following section.

513 The sediment regime of the stream is not characterized by a constant sediment supply,
514 but rather by the episodic occurrence of rainfall events and subsequent high stream flow.
515 During high rainfall events, all catchment compartments may be actively connected to the
516 mainstream (Bracken et al., 2015; Gomi et al., 2008). Given that sediment sources are well-
517 connected to the stream, large events can transport sediment directly from eroded hillslopes
518 and even flush previously deposited sediment (Le Gall et al., 2017). Hence, such event-based
519 sediment samples provide robust information about sediment source hotspots at the catchment
520 scale. Our estimations corroborated that DF is highly vulnerable to water erosion.
521 Additionally, the 2015 Gorkha earthquake event might have damaged the steep hillslope
522 surface of forested areas and subsequently triggered high sediment generation. The lack of
523 landslides in the forest, the predominance of the bedrock dominated stream and relatively
524 intact and dense vegetation cover during summer suggest that steep topography and high-

525 intensity rainfall might be major controlling physical factors for sediment generation and
526 mobilization from the hillslope forested areas of this catchment.

527

528 **4.3 Controls on sediment sources: land management activities**

529 Despite the traditional view of a dominant sediment contribution from agricultural
530 fields, Pooled-MixSIAR showed that agriculture contributed <5% to suspended sediments at
531 the outlet of Chitlang stream (Fig. 5). Our results are in line with those of previous studies in
532 the mid-hill catchments with terraced agriculture (Brown et al., 1999; Carver, 1997; Slaets et
533 al., 2016). However, the Pooled-MixSIAR approach tends to average the variation of tracers
534 of land uses located within different sub-catchments. Consequently, it provides source
535 contribution results with high uncertainty. Furthermore, significant errors could be introduced
536 if source groups are classified on the basis of catchment-wide generic sources alone in a
537 catchment with heterogeneous vegetation and terrain (Pulley et al., 2017). In contrast, D-
538 MixSIAR uses stratified source samples, which accounts for tracer variability of sources
539 within individual sub-catchments and allows weighting of mixture proportions by sub-
540 catchment contributions. The approach relies on the nested structure of the drainage network,
541 therefore, reducing the complexity of tracer signatures of different sources within individual
542 sub-catchments. As a result, within-source tracer variability decreased and discrimination of
543 sources increased (Fig. A.8).

544 Combining total sub-catchment estimates with land use contributions computed for each
545 tributary sub-catchment provides the basis for calculating weighted source contribution via D-
546 MixSIAR along the catchment cascade (M3, M5, M6 sediment). We used D-MixSIAR to
547 estimate land use contributions to suspended sediments. The contribution from BLF, RT-1
548 and UP-E decreased downstream ($M3 > M5 > M6$) as sediment transport distance from the
549 location of the sources increases (Fig. A.7). The contribution of MF increased downstream

550 until M5 and remained stable towards the catchment outlet (M6). Based on D-MixSIAR, the
551 majority of sediment originated from MF, followed by BLF and RT-1 at the outlet of
552 catchment (Fig. 6, Fig.A.7), indicating that there is no *a priori* basis for assuming that
553 forested areas have inherently low rates of sediment generation even if forest land was
554 reported to have a low soil erodibility factor (Upadhayay et al., 2014). The increasing
555 contribution of MF along the sediment cascade can be explained by disturbed MF soil surface
556 on the steep slopes due to the impact of livestock grazing and collection of leaf litter using
557 hoe. D-MixSIAR results were consistent with the conceptual understanding of the catchment
558 (distribution of land use with slope gradient) and could be justified by the qualitative data. In
559 a survey of 150 households from an upstream village within the larger Kulekhani catchment
560 in 2013 (Panta et al., 2014), a majority (64%) of the farmers perceived that deforestation was
561 the main reason for soil erosion followed by road construction (28%), while only a minority
562 (2%) noted both unmanaged cropping pattern and stream bank erosion as major contributors
563 of sediments to the Kulekhani reservoirs.

564 Agriculture is predicted to be a minor source of sediment (mean contribution 15 - 20%)
565 input to the Chitlang stream network. The low contribution of agricultural terraces to the
566 sediment can probably be attributed to proper terrace maintenance and traditional irrigation
567 systems (Brown et al., 1999; Carver, 1997). Local farmers use back-sloping bench terraces for
568 upland agriculture with ditches around the terraces to direct the surface runoff out of the
569 upland terraces, thereby decreasing rill and ephemeral gully formation on agricultural fields.
570 In addition, most of the eroded soil from upland terraces is finally transferred to irrigated
571 lowland terraces through run-on as well as through irrigation water and deposited on the
572 irrigated terraces as well as the canal bed. Carver (1997) estimated an accumulation of 6.6
573 mm year⁻¹ of eroded material on the irrigated terraces in the mid-hills of Nepal. The authors
574 observed that deposited sediment was frequently cleaned from irrigation canals. Thus,

575 irrigation canals and terracing slow down sediment transfer and result in upstream
576 accumulation of sediment on the valley floor and lowland terrace, forming local net sediment
577 sink zones modifying the sediment dynamics at the catchment scale (Brown et al., 1999;
578 Carver, 1997).

579 D-MixSIAR results showed that forests (BLF and MF) were the primary sediment source
580 during all seasons while unpaved road tracks represented a major secondary sediment source
581 within the Chitlang catchment. Soil erosion in the forest might be exacerbated by the
582 combination of surface disturbance (e.g. leaf litter collection activities), high rainfall intensity,
583 seasonally dry periods, forest fires and naturally dynamic landscapes. The short-duration,
584 high-intensity monsoon storms that are common in the catchment provide the required rainfall
585 erosivity to initiate surface erosion on steeper slopes (Bookhagen, 2010; Karki et al., 2017).
586 Farmers collect leaf litter using hand racking, harvest timber and graze livestock (cows and
587 goats) in the forest, which makes the forest floor bare or disturbed. Gardner and Gerrard
588 (2002) suggested that ground cover is more important than canopy cover in reducing runoff
589 and water erosion in the mid-hill forest. The average rate of soil loss and the contribution to
590 total soil loss from steeper slopes are tremendously high compared with that from gentle
591 slopes (Bahadur, 2012; Garcia-Ruiz et al., 2015; Su et al., 2016). Moreover, unfortified dirt
592 roads located inside the broadleaf forest are highly vulnerable to erosion due to rutted surfaces.
593 Most of the rural roads in the mid-hills are unpaved and poorly maintained without roadside
594 drainage systems, leading to concentrated flow, resulting in soil erosion (Merz et al., 2006; Su
595 et al., 2016). Additional tracers such as fallout radionuclides may provide further insight into
596 the major erosion processes generating sediment from different land uses, which is lacking in
597 this study. Notwithstanding, the continued supply of sediment from forests will result in rapid
598 siltation of the reservoir and loss of ecosystem services that consequently result in shortened
599 economic returns from the reservoir. Thus, in order to protect the catchment from degradation,

600 forests should be better managed. However, since decisions to protect the forests are enforced
601 by the community forest user groups (CFUs), the planning of effective measures for soil
602 conservation in the forests should target a ‘bottom-up’ approach. This should ideally involve
603 the integration of CFUs in a framework of paying for ecosystem services, performance-based
604 disbursement of electricity revenue to local communities, and effective monitoring of forest
605 and other developmental activities (e.g. road construction) across the catchment.

606

607 **5 Conclusions**

608 The stable carbon isotopic composition of long-chain saturated FAs ($\delta^{13}\text{C}$ -FA) associated
609 with soil of various land uses and different types of stream sediment (bed, suspended, event)
610 were used as input for a Bayesian mixing model to estimate the spatio-temporal variation in
611 land use-specific sediment source contributions to the Chitlang stream located in the mid-hills
612 of Nepal. We showed that applying catchment-wide (generic) sources cannot explain the
613 sediment transport within the catchment because sediment delivery from the different sources
614 is sub-catchment specific due to localized changes in gradient, ground cover, vegetation and
615 microtopography in the mountaneous catchments. Application of a deconvolutional
616 framework to MixSIAR (D-MixSIAR) strongly enhanced our understanding of the relatively
617 complex patterns of sediment contributions to different tributaries representing sub-
618 catchments along the mainstream. This study showed that the largest sources of sediment in
619 Chitlang catchment were mixed forest (MF) ($41 \pm 13\%$) and broadleaf forest (BLF) ($15 \pm 8\%$)
620 followed by unpaved rural road tracks on flat ($11 \pm 8\%$) and steep lands ($9 \pm 7\%$) during early
621 wet season (the time of highest risk for soil erosion by water in the mid-hills of Nepal). The
622 effect of temporal hydrological variability on the land use contributions was not significant.
623 Clearly, sediment sources showed high spatial variation along the Chitlang stream sediment

624 cascade because of spatial changes in topography and land use management. Prediction of
625 source contributions was improved by a categorization of sources for each sub-catchment and
626 estimation of a total, weighted source contribution using sub-catchment contributions.

627 Overall this study showed that community managed forest is the major primary, and road
628 tracks are dominant secondary sources of sediments at the different locations of Chitlang
629 stream. The estimates of agricultural terraces contribution are significantly lower compared
630 to forest throughout the year. It is acknowledged that D-MixSIAR is still a black-box model
631 that provides no information on the internal processes, or secondary sediment sources and
632 sinks within the catchment. Therefore, without spatially explicit sediment loading data,
633 proportions must still be compared with some caution. Nevertheless, management of forests
634 and unpaved roads in the Chitlang catchment should be an essential component of the
635 strategies to control sediment inputs to Kulekhani reservoir. Hence, there is a need for better
636 coordination among community forest user groups and provision of hydroelectricity revenue
637 in return for forest conservation measures.

638

639 Acknowledgements

640 This work was financially supported by Vlaamse Inter-universitaire Raad (VLIR)
641 Belgium as a part of an ICP-PhD grant. Special thank is expressed to the Horizon 2020, RISE
642 IMIXSED (Integrating isotopic techniques with Bayesian modelling for improved assessment
643 and management of global sedimentation problems) project for MixSIAR training. We are
644 very grateful for the comments made by the anonymous reviewer and we believe that they
645 have helped us to significantly improve the manuscript.

646

647 References

- 648 Acharya GP, Tripathi BP, Gardner RM, Mawdesley KJ, McDonald MA. Sustainability of
649 sloping land cultivation systems in the mid-hills of Nepal. *Land Degradation &*
650 *Development* 2008; 19: 530-541.
- 651 Bahadur KCK. Spatio-temporal patterns of agricultural expansion and its effect on watershed
652 degradation: a case from the mountains of Nepal. *Environmental Earth Sciences* 2012;
653 65: 2063-2077.
- 654 Benner R, Fogel ML, Sprague EK, Hodson RE. Depletion of C-13 in lignin and its
655 implications for stable carbon isotope studies. *Nature* 1987; 329: 708-710.
- 656 Blake WH, Ficken KJ, Taylor P, Russell MA, Walling DE. Tracing crop-specific sediment
657 sources in agricultural catchments. *Geomorphology* 2012; 139: 322-329.
- 658 Bookhagen B. Appearance of extreme monsoonal rainfall events and their impact on erosion
659 in the Himalaya. *Geomatics Natural Hazards & Risk* 2010; 1: 37-50.
- 660 Bracken LJ, Turnbull L, Wainwright J, Bogaart P. Sediment connectivity: a framework for
661 understanding sediment transfer at multiple scales. *Earth Surface Processes and*
662 *Landforms* 2015; 40: 177-188.
- 663 Brown S, Schreier H, Shah PB, Lavkulich LM. Modelling of soil nutrient budgets: an
664 assessment of agricultural sustainability in Nepal. *Soil Use and Management* 1999; 15:
665 101-108.
- 666 Carver M. Diagnosis of Headwater Sediment Dynamics in Nepal's Middle Mountains:
667 Implications for Land Management. PhD thesis. University of British Columbia,
668 Vancouver, Canada, 1997.
- 669 Collins AL, Pulley S, Foster IDL, Gellis A, Porto P, Horowitz AJ. Sediment source
670 fingerprinting as an aid to catchment management: a review of the current state of
671 knowledge and a methodological decision-tree for end-users. *Journal of*
672 *Environmental Management* 2017; 194: 86-108.
- 673 Collins AL, Williams LJ, Zhang YS, Marius M, Dungait JAJ, Smallman DJ, Dixon ER,
674 Stringfellow A, Sear DA, Jones JI, Naden PS. Catchment source contributions to the
675 sediment-bound organic matter degrading salmonid spawning gravels in a lowland
676 river, southern England. *Science of The Total Environment* 2013; 456-457: 181-195.
- 677 Collins AL, Williams LJ, Zhang YS, Marius M, Dungait JAJ, Smallman DJ, Dixon ER,
678 Stringfellow A, Sear DA, Jones JI, Naden PS. Sources of sediment-bound organic
679 matter infiltrating spawning gravels during the incubation and emergence life stages of
680 salmonids. *Agriculture Ecosystems & Environment* 2014; 196: 76-93.
- 681 Cooper RJ, Krueger T, Hiscock KM, Rawlins BG. High-temporal resolution fluvial sediment
682 source fingerprinting with uncertainty: a Bayesian approach. *Earth Surface Processes*
683 *and Landforms* 2015; 40: 78-92.
- 684 Davis P, Syme J, Heikoop J, Fessenden-Rahn J, Perkins G, Newman B, Chrystal AE, Hagerty
685 SB. Quantifying uncertainty in stable isotope mixing models. *Journal of Geophysical*
686 *Research-Biogeosciences* 2015; 120: 903-923.
- 687 Dhital MR. *Geology of the Nepal Himalaya: regional perspective of the classic collided*
688 *Orogen*. London: Springer, 2015.
- 689 Diefendorf AF, Leslie AB, Wing SL. Leaf wax composition and carbon isotopes vary among
690 major conifer groups. *Geochimica Et Cosmochimica Acta* 2015; 170: 145-156.
- 691 Dijkshoorn K, Huting J. Soil and terrain database for Nepal. Report No: Report 2009/01,
692 (available through: <http://www.isric.org>), ISRIC-World Soil Information,
693 Wageningen, The Netherland (29 p. with data set). 2009.
- 694

695 Fine ST, Carter BJ. Effect of Sedimentation on Soil Organic Carbon Content and delta 13C
696 Values After 7 Years of Burial. *Soil Science* 2013; 178: 647-653.

697 Fox JF, Ford WI. Impact of landscape disturbance on the quality of terrestrial sediment
698 carbon in temperate streams. *Journal of Hydrology* 2016; 540: 1030-1042.

699 Fox JF, Martin DK. Sediment fingerprinting for calibrating a soil erosion and sediment-yield
700 model in mixed land-use watersheds. *Journal of Hydrologic Engineering* 2015; 20:
701 C4014002-1

702 Fox JF, Papanicolaou AN. The use of carbon and nitrogen isotopes to study watershed erosion
703 processes. *Journal of the American Water Resources Association* 2007; 43: 1047-1064.

704 Garcia-Ruiz JM, Begueria S, Nadal-Romero E, Gonzalez-Hidalgo JC, Lana-Renault N,
705 Sanjuan Y. A meta-analysis of soil erosion rates across the world. *Geomorphology*
706 2015; 239: 160-173.

707 Gardner RAM, Gerrard AJ. Relationships between runoff and land degradation on non-
708 cultivated land in the Middle Hills of Nepal. *International Journal of Sustainable*
709 *Development and World Ecology* 2002; 9: 59-73.

710 Gardner RAM, Gerrard AJ. Runoff and soil erosion on cultivated rainfed terraces in the
711 Middle Hills of Nepal. *Applied Geography* 2003; 23: 23-45.

712 Gibbs MM. Identifying source soils in contemporary estuarine sediments: a new compound-
713 specific isotope method. *Estuaries and Coasts* 2008; 31: 344-359.

714 Gibbs MM. Protocols on the use of the CSSI technique to identify and apportion soil sources
715 from land use Report No: HAM2013-106, National Institute of Water and
716 Atmospheric Research Ltd, Hamilton, New Zealand. 2013.

717 Gomi T, Sidle RC, Miyata S, Kosugi K, Onda Y. Dynamic runoff connectivity of overland
718 flow on steep forested hillslopes: Scale effects and runoff transfer. *Water Resources*
719 *Research* 2008; 44: W08411.

720 GoN/EbA/UNDP. Development of Ecosystem based Sediment Control Techniques and
721 Design of Siltation Dam to Protect Phewa Lake. Report No, Summary Report.
722 Prepared By Forum for Energy and Environment Development (FEED) P. Ltd. for
723 The Ecosystem Based Adaptation in Mountain Ecosystems (EbA) Nepal Project.
724 Government Of Nepal, United Nations Environment Programme, United Nations
725 Development Programme, International Union For Conservation Of Nature, and the
726 German Federal Ministry for the Environment, Nature Conservation, Building And
727 Nuclear Safety. 2015.

728 Griepentrog M, Eglinton TI, Hagedorn F, Schmidt MWI, Wiesenberg GLB. Interactive
729 effects of elevated CO₂ and nitrogen deposition on fatty acid molecular and isotope
730 composition of above- and belowground tree biomass and forest soil fractions. *Global*
731 *Change Biology* 2015, 21: 473-486.

732 Hancock GJ, Revill AT. Erosion source discrimination in a rural Australian catchment using
733 compound-specific isotope analysis (CSIA). *Hydrological Processes* 2013; 27: 923-
734 932.

735 Hardy F, Bariteau L, Lorrain S, Theriault I, Gagnon G, Messier D, Rougerie JF. Geochemical
736 tracing and spatial evolution of the sediment bed load of the Romaine River, Quebec,
737 Canada. *Catena* 2010; 81: 66-76.

738 Huberty CJ, Olejnik S. *Applied MANOVA and Discriminant Analysis*: Wiley, 2006.

739 Ichihara K, Fukubayashi Y. Preparation of fatty acid methyl esters for gas-liquid
740 chromatography. *Journal of Lipid Research* 2010; 51: 635-640.

741 Jackson A. SIBER. Web <https://github.com/AndrewLJackson/SIBER>. Accessed. 15 July,
742 2016.

743 Jandl G, Leinweber P, Schulten HR. Origin and fate of soil lipids in a Phaeozem under rye
744 and maize monoculture in Central Germany. *Biology and Fertility of Soils* 2007; 43:
745 321-332.

746 Jandl G, Leinweber P, Schulten HR, Ekschmitt K. Contribution of primary organic matter to
747 the fatty acid pool in agricultural soils. *Soil Biology & Biochemistry* 2005; 37: 1033-
748 1041.

749 Karki R, ul Hasson S, Schickhoff U, Scholten T, Bohner J. Rising Precipitation Extremes
750 across Nepal. *Climate* 2017; 5: 4.

751 Koiter AJ, Lobb DA, Owens PN, Petticrew EL, Tiessen KHD, Li S. Investigating the role of
752 connectivity and scale in assessing the sources of sediment in an agricultural
753 watershed in the Canadian prairies using sediment source fingerprinting. *Journal of*
754 *Soils and Sediments* 2013a; 13: 1676-1691.

755 Koiter AJ, Owens PN, Petticrew EL, Lobb DA. The behavioural characteristics of sediment
756 properties and their implications for sediment fingerprinting as an approach for
757 identifying sediment sources in river basins. *Earth-Science Reviews* 2013b; 125: 24-
758 42.

759 Laceby JP, Olley J, Pietsch TJ, Sheldon F, Bunn SE. Identifying subsoil sediment sources
760 with carbon and nitrogen stable isotope ratios. *Hydrological Processes* 2015; 29: 1956-
761 1971.

762 Lamba J, Karthikeyan KG, Thompson AM. Apportionment of suspended sediment sources in
763 an agricultural watershed using sediment fingerprinting. *Geoderma* 2015; 239: 25-33.

764 Le Gall M, Evrard O, Foucher A, Laceby JP, Salvador-Blanes S, Maniere L, Lefevre I,
765 Cerdan O, Ayrault S. Investigating the temporal dynamics of suspended sediment
766 during flood events with Be-7 and Pb-210(xs) measurements in a drained lowland
767 catchment. *Scientific Reports* 2017; 7: 42099

768 McCarney-Castle K, Childress TM, Heaton CR. Sediment source identification and load
769 prediction in a mixed-use Piedmont watershed, South Carolina. *Journal of*
770 *Environmental Management* 2017; 185: 60-69.

771 McFerrin L. HDMD: Statistical analysis tools for high dimension molecular data (HDMD). R
772 package version 1.2. <https://CRAN.R-project.org/package=HDMD> 2013.

773 Merz J. Water balances, floods and sediment transport in the Hindu Kush-Himalayas. Web
774 <http://lib.icimod.org/record/7484>. Accessed. 22 March, 2017.

775 Merz J, Dangol PM, Dhakal MP, Dongol BS, Nakarmi G, Weingartner R. Road construction
776 impacts on stream suspended sediment loads in a nested catchment system in Nepal.
777 *Land Degradation & Development* 2006; 17: 343-351.

778 Mukundan R, Walling DE, Gellis AC, Slattery MC, Radcliffe DE. Sediment source
779 fingerprinting: transforming from a research tool to a management tool. *Journal of the*
780 *American Water Resources Association* 2012; 48: 1241-1257.

781 NEA. A Year in review-fiscal year 2015/2016. Report No, Nepal Electricity Authority,
782 Kathmandu, Nepal. 2016.

783 Panta D, Rao N, Upadhyay SN, Karky BS. Benefit sharing mechanisms in hydropower
784 projects: Lessons from Nepal and India. In: Vaidya RA, Sharma E, editors. *Research*
785 *Insights on climate and water in the Hindu Kush Himalayas*. ICIMOD, Kathmandu,
786 Nepal 2014.

787 Parnell AC, Inger R, Bearhop S, Jackson AL. Source partitioning using stable isotopes:
788 coping with too much variation. *PLoS One* 2010; 5: e9672.

789 Phillips DL, Gregg JW. Uncertainty in source partitioning using stable isotopes. *Oecologia*
790 2001; 127: 171-179.

791 Phillips JM, Russell MA, Walling DE. Time-integrated sampling of fluvial suspended
792 sediment: a simple methodology for small catchments. *Hydrological Processes* 2000;
793 14: 2589-2602.

794 Pulley S, Foster I, Collins AL. The impact of catchment source group classification on the
795 accuracy of sediment fingerprinting outputs. *Journal of Environmental Management*
796 2017; 194: 16-26.

797 Semmens BX, Ward EJ, Moore JW, Darimont CT. Quantifying inter- and intra-population
798 niche variability using hierarchical Bayesian stable isotope mixing models. *PLoS One*
799 2009; 4: e6187.

800 Shrestha HS. Sedimentation and sediment handling in himalayan reservoirs. Department of
801 Hydraulics and Environmental Engineering. PhD thesis. Norwegian University of
802 Science and Technology, Trondheim, Norway, 2012, pp. 236.

803 Slaets JIF, Schmitter P, Hilger T, Hue DTT, Piepho HP, Vien TD, Cadisch G. Sediment-
804 associated organic carbon and nitrogen inputs from erosion and irrigation to rice fields
805 in a mountainous watershed in Northwest Vietnam. *Biogeochemistry* 2016; 129: 93-
806 113.

807 Stewart HA, Massoudieh A, Gellis A. Sediment source apportionment in Laurel Hill Creek,
808 PA, using Bayesian chemical mass balance and isotope fingerprinting. *Hydrological*
809 *Processes* 2015; 29: 2545-2560.

810 Sthapit KM, Balla MK. Review of runoff and soil loss studies: A teching material. Institute of
811 forestry (IOF), Pokhara, Nepal, 1998.

812 Stock BC, Semmens BX. MixSIAR GUI User Manuel. Version 3.1. Web
813 <https://github.com/brianstock/MixSIAR/>. Accessed. 26 February, 2016.

814 Su Z-a, Xiong D-h, Deng W, Dong Y-f, Ma J, Padma CP, Gurung BS. ¹³⁷Cs tracing
815 dynamics of soil erosion, organic carbon, and total nitrogen in terraced fields and
816 forestland in the Middle Mountains of Nepal. *Journal of Mountain Science* 2016; 13:
817 1829-1839.

818 Tiwari KR, Sitaula BK, Bajracharya RM, Borresen T. Runoff and soil loss responses to
819 rainfall, land use, terracing and management practices in the Middle Mountains of
820 Nepal. *Acta Agriculturae Scandinavica Section B-Soil and Plant Science* 2009; 59:
821 197-207.

822 Upadhayay HR, Bodé S, Griepentrog M, Bajracharya RM, Blake W, Cornelis W, Boeckx P.
823 Isotope mixing models require individual isotopic tracer content for correct
824 quantification of sediment source contributions. *Hydrological Processes* 2018; 32:
825 981-989.

826 Upadhayay HR, Bodé S, Griepentrog M, Huygens D, Bajracharya RM, Blake WH, Dercon G,
827 Mabit L, Gibbs M, Semmens BX, Stock BC, Cornelis W, Boeckx P. Methodological
828 perspectives on the application of compound-specific stable isotope fingerprinting for
829 sediment source apportionment. *Journal of Soils and Sediments* 2017; 17: 1537-1553.

830 Upadhayay HR, Gajurel S, Bajaracharya RM, Cornelis W, Boeckx P. Effect of land use on
831 soil degradation in Chitlang watershed of Nepal. *Forestry (Journal of Institute of*
832 *Forestry, Nepal)* 2014; 14: 28-41.

833 Vale SS, Fuller IC, Procter JN, Basher LR, Smith IE. Application of a confluence-based
834 sediment-fingerprinting approach to a dynamic sedimentary catchment, New Zealand.
835 *Hydrological Processes* 2016; 30: 812-829.

836 Venables WN, Ripley BD. *Modern applied statistics with S*. New York: Springer, 2002.

837 Vercruyse K, Grabowski RC, Rickson RJ. Suspended sediment transport dynamics in rivers:
838 Multi-scale drivers of temporal variation. *Earth-Science Reviews* 2017; 166: 38-52.

839 von Westarp S, Schreier H, Brown S, Shah RB. Agricultural intensification and the impacts
840 on soil fertility in the Middle Mountains of Nepal. *Canadian Journal of Soil Science*
841 2004; 84: 323-332.
842 Walling DE. The evolution of sediment source fingerprinting investigations in fluvial systems.
843 *Journal of Soils and Sediments* 2013; 13: 1658-1675.
844 Wilkinson SN, Olley JM, Furuichi T, Burton J, Kinsey-Henderson AE. Sediment source
845 tracing with stratified sampling and weightings based on spatial gradients in soil
846 erosion. *Journal of Soils and Sediments* 2015; 15: 2038-2051.
847

848

849

850

851

852

853

854

855

856

857

858

859

860

861

862

863

864 Tables

865 Table 1 Characteristics of sediment sampling locations (see Fig. 1) and potential sediment
866 sources (broad leaf forest (BLF), mixed forest (MF), pine forest (PF), encroached upland
867 terraces into BLF (UP-E), upland terraces (UP), lowland terraces (LL)), unpaved road tracks
868 on slopes inside BLF (RT-1) and unpaved road tracks on flatter areas (RT)).

869 Table 2 Mahalanobis distances between group centroids (see Fig. 4) and reliability of source
870 discrimination analysis using $\delta^{13}\text{C}$ of long-chain saturated fatty acids ($\text{C}_{22}\text{-C}_{32}$). Significant
871 effects are in bold. Sources: broad leaf forest (BLF), mixed forest (MF), pine forest (PF),
872 upland terraces (UP), lowland terraces (LL), unpaved road tracks (RT).

873 Table 3 Sediment source apportionment after a high rainfall event (14 to 15 August, 2014) and
874 aftershocks following the Gorkha earthquake (7.8 M) on 25 April 2015. Abbreviations:
875 deciduous forest (DF), broad leaf forest (BLF), mixed forest (MF), combined agriculture
876 terraces (AG), lowland terraces (LL), upland terraces (UP), pine forest (PF), unpaved road
877 tracks (RT).

878 Table 4 Estimated relative contribution of each tributary sub-catchments (M1 = Dandakharka,
879 M2 = Kharka, M3 = Upper-Chitlang and M4 = Chhabugaun) to the confluence-sediment (M3,
880 M5) for early, mid and late wet season. For details see Figures 1 and 6. Mean \pm standard
881 deviation with 90% credible intervals in parenthesis.

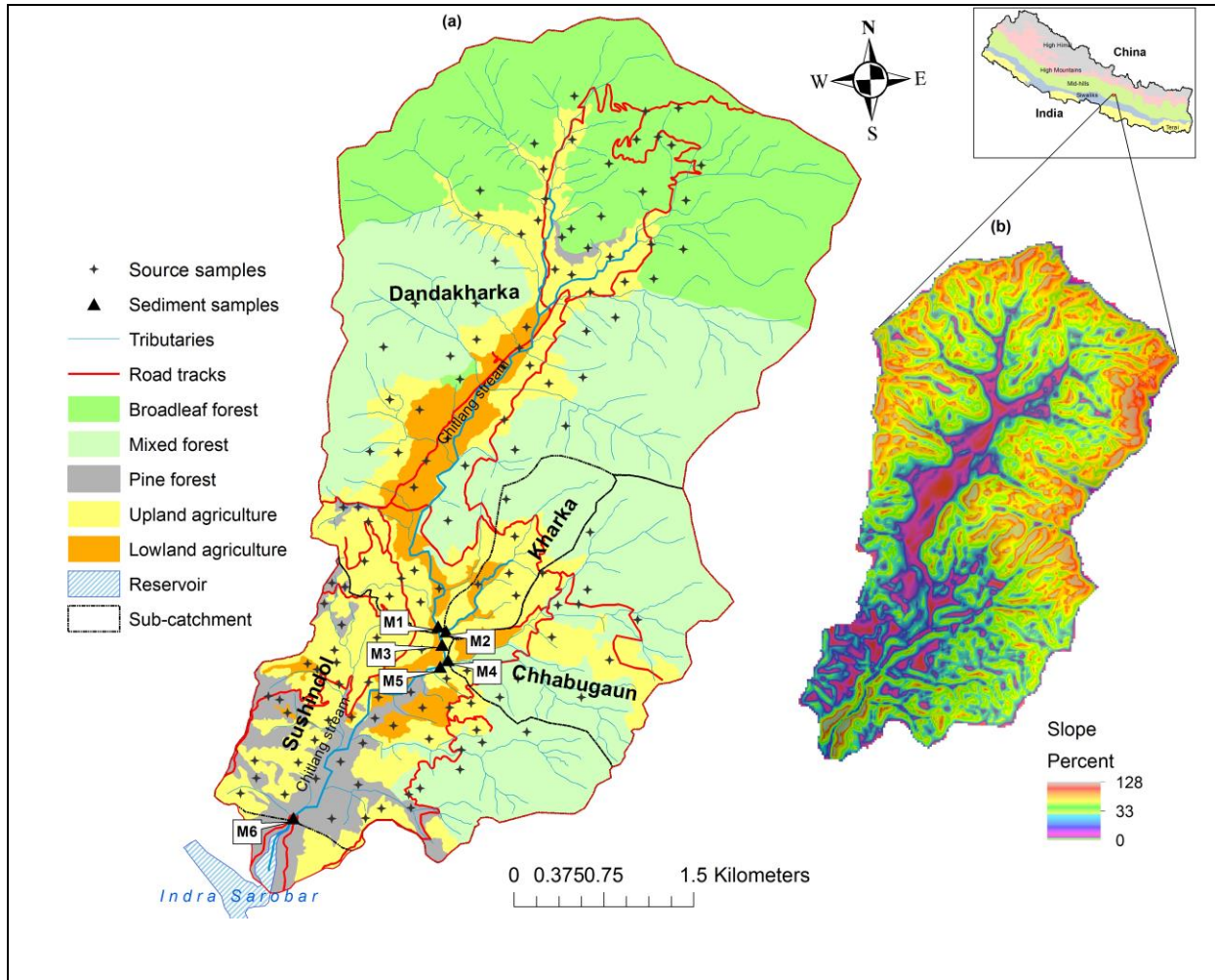
882

883

884

885

886 Figures



887

888 Fig. 1 Chitlang catchment in the mid-hills of Nepal (upper-right inset) (a) sub-catchments,
889 land use and land cover distributions (digitized from **Google Earth**) with source and sediment
890 (M1, M2, M3, M4, M5 and M6) sampling locations, and (b) slope map of the study area
891 obtained from digitized map layers of topographic map published by the Department of
892 Survey, Government of Nepal (1996).

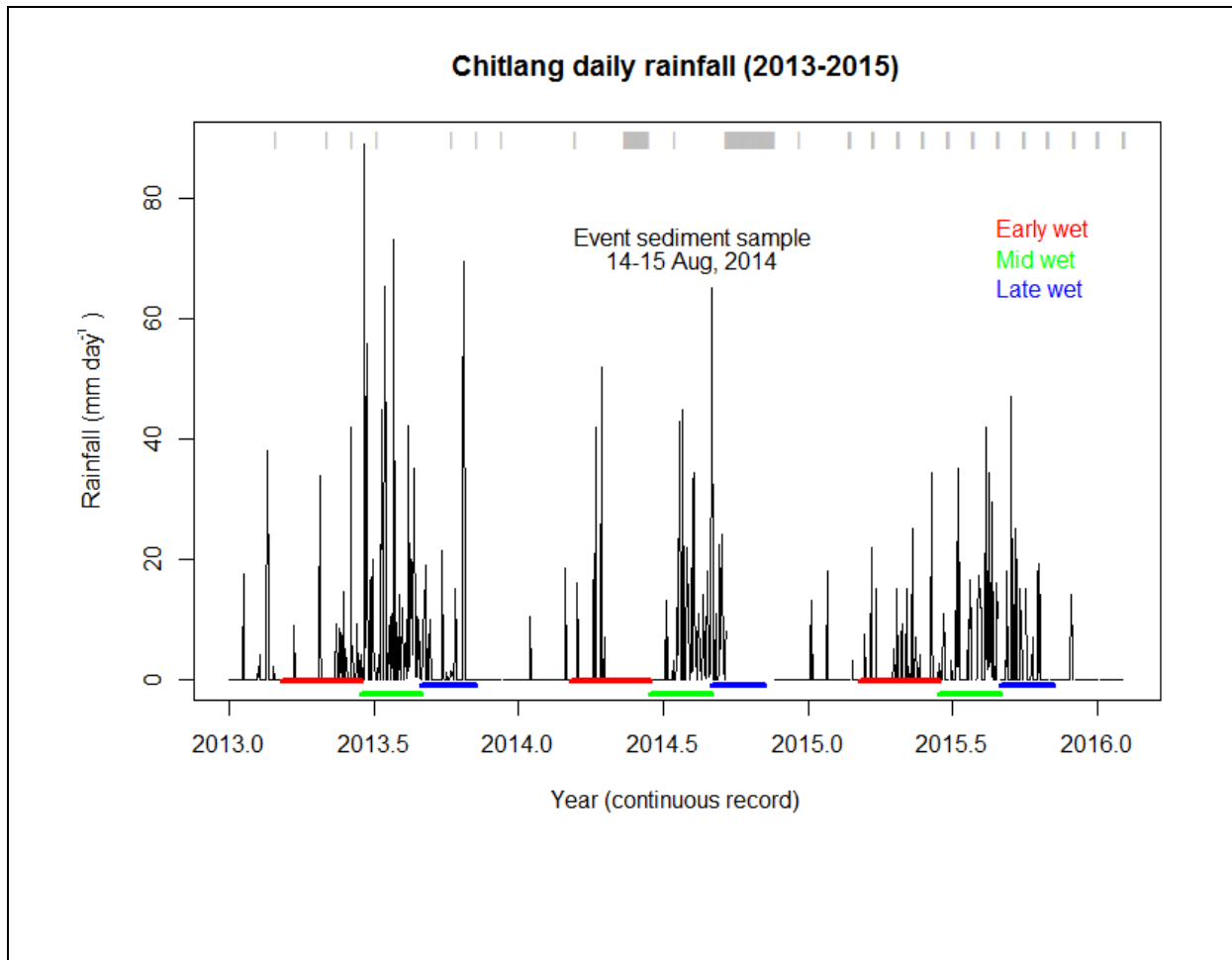
893

894



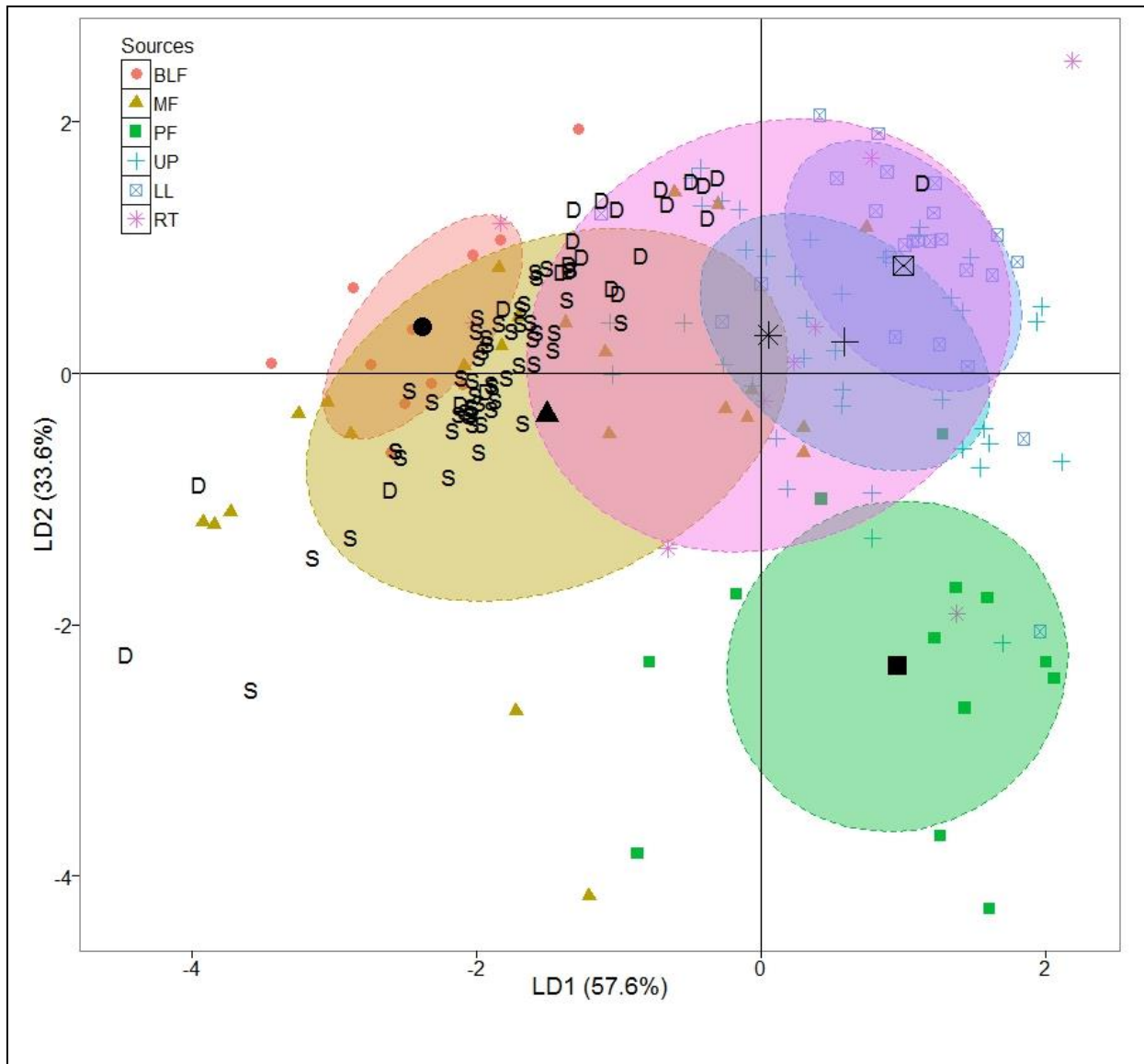
895

896 Fig. 2 Source soil and sediment sampling in the Chitlang catchment, (a) mixed rain-fed and
897 irrigated farming on terraces (middle) and mixed forest on steep slopes (left and right), (b)
898 stream bed sediment sampling with flat trowel and (c) installed time-integrated mass-flux
899 sampler (TIMS) at the outlet of the Chitlang stream.



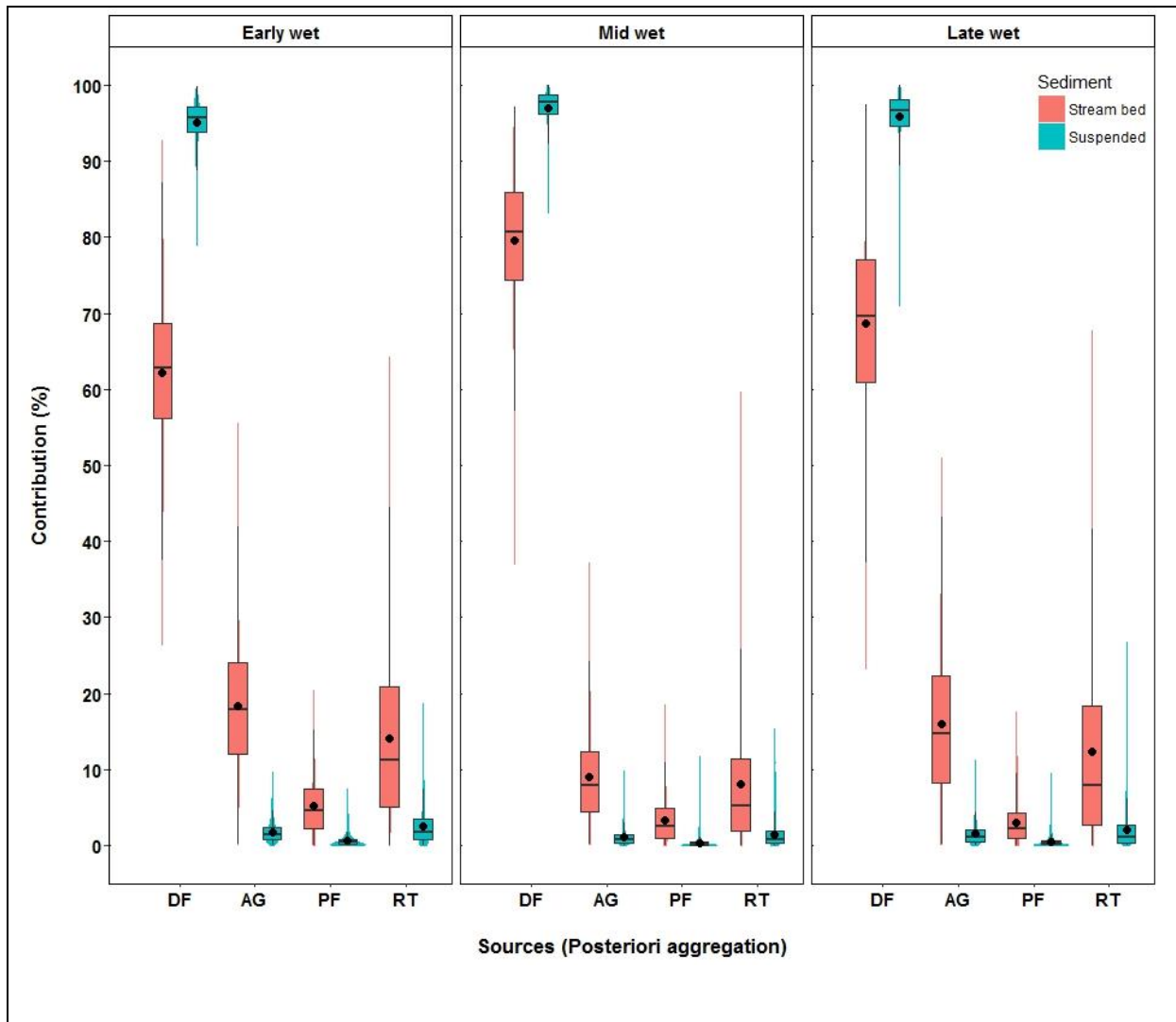
900

901 Fig. 3 Rainfall distribution in Markhu station (Index no. 0915, Department of Hydrology and
 902 Meteorology, Government of Nepal) at the outlet of Chitlang catchment. Horizontal gray bars
 903 on top represent missing rainfall data while bottom horizontal bars represent sediment
 904 sampling periods (red = early wet, green = mid wet and blue = late wet periods).



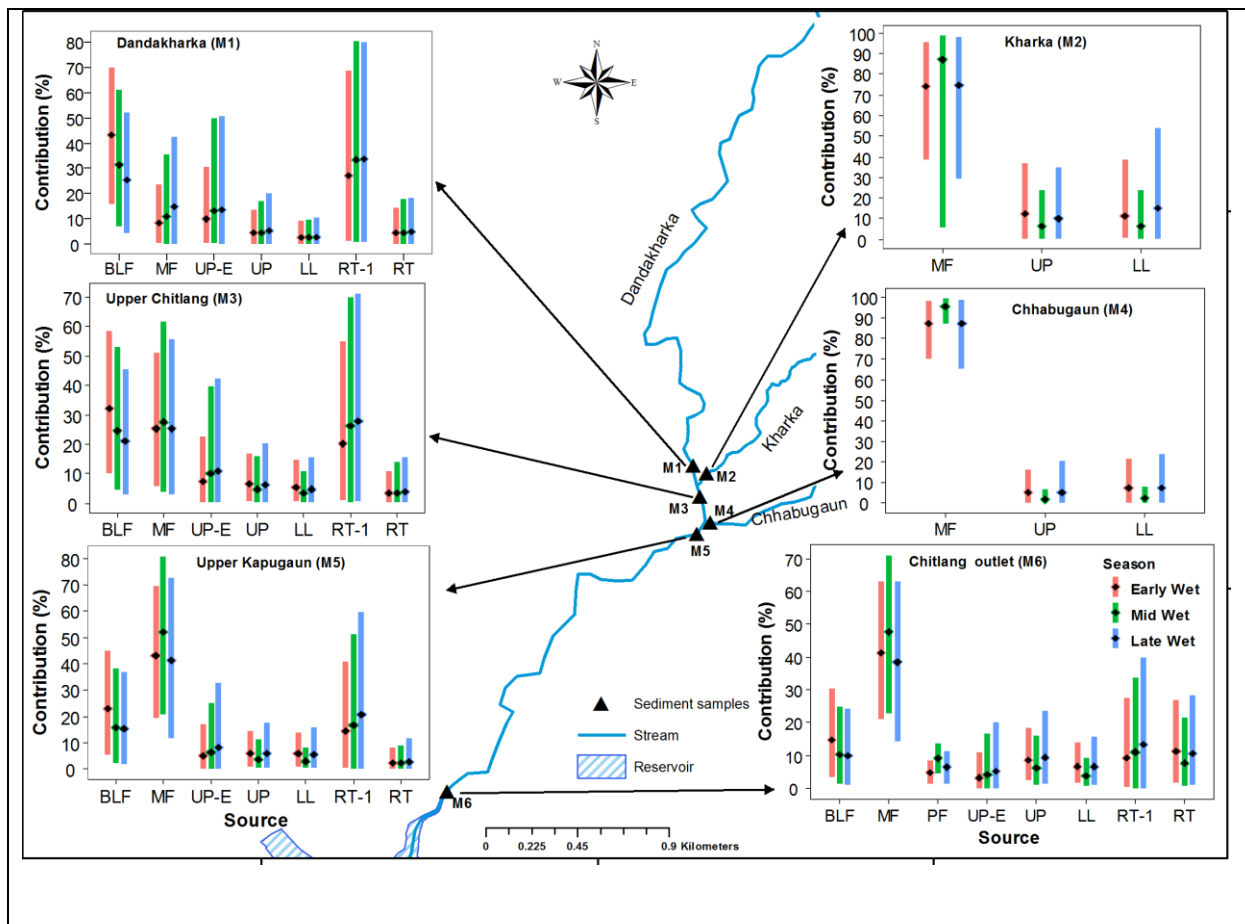
905

906 Fig. 4 Discriminant analysis (DA) of generic sediment sources using $\delta^{13}\text{C}$ of saturated long-
 907 chain fatty acids ($\text{C}_{22}\text{-C}_{32}$) with projection of sediment samples (S = suspended and D =
 908 stream bed) on the LDA scatter plot. Shaded ellipsoids encompass 50% of group variability.
 909 Sources: broad leaf forest (BLF), mixed forest (MF), pine forest (PF), upland terraces (UP),
 910 lowland terraces (LL), unpaved road tracks (RT).



911

912 Fig. 5 Source contributions to streambed and suspended sediments at the catchment outlet
 913 estimated based on $\delta^{13}\text{C}$ FA tracers (C_{22} - C_{32}) using concentration-dependent pooled-
 914 MixSIAR model. Box plots with solid circle representing the average contribution. Sources:
 915 deciduous forest (DF), agricultural terraces (AG), pine forest (PF) and unpaved road tracks
 916 (RT).



917

918 Fig. 6 Mean relative contribution (%) of sediment sources estimated with deconvolutional
 919 MixSIAR using confluence-based suspended sediment collected before and after confluences
 920 at different tributaries of Chitlang stream. Vertical bars represent 90% credible intervals and
 921 the middle point (black diamond) represents the average contribution, while seasons are given
 922 in different colours. Sources: broadleaf forest (BLF), mixed forest (MF), pine forest (PF),
 923 encroached upland terraces into BLF (UP-E), upland terraces (UP), lowland terraces (LL),
 924 unpaved road tracks on slope inside BLF (RT-1) and unpaved road tracks on flat terrain (RT).

925